Biomicrofluidics ARTICLE scitation.org/journal/bmf

Accomplishment of one-step specific PCR and evaluated SELEX process by a dual-microfluidic amplified system

Cite as: Biomicrofluidics 15, 024107 (2021); doi: 10.1063/5.0045965
Submitted: 30 January 2021 · Accepted: 22 March 2021 ·
Published Online: 5 April 2021

Jing Chen,[1] Xiaohui Liu,[1] Meng Xu,[1] Zhoumin Li,[2] and Danke Xu[1,a)]

AFFILIATIONS

[1]State Key Laboratory of Analytical Chemistry for Life Science, School of Chemistry and Chemical Engineering, Nanjing University, Nanjing 210023, China
[2]Jinling College, Nanjing University, Nanjing 210089, China

[a)]**Author to whom correspondence should be addressed:** xudanke@nju.edu.cn

ABSTRACT

One of the main obstacles for systematic evolution of ligands by exponential enrichment (SELEX) failure is the generation of a non-specific product, as selection-inherent amplification procedures tend to form by-products, which prevents the enrichment of target-binding aptamers. Herein, we reported a dual-microfluidic amplified system (dual-MAS) based on the real-time polymerase chain reaction (PCR) detection chip and the large volume PCR chip for one-step specific PCR and for evaluating the SELEX process. First, it is a simple method to accomplish analytical PCR and amplification PCR in one step, and the optimal number of cycles for generating the specific PCR product is the cycles when the slope of the linear amplification period of the real-time PCR curve begins to decrease. Second, the time used by the dual-MAS for generating a specific PCR product is reduced to 30 min, and the multi-functional dual-MAS can simultaneously evaluate the SELEX process by providing important information on the amounts of enriched sequences and the library diversity in every round of SELEX. In addition, pollution contamination and fragment loss can be significantly avoided in the closed chip. Last, the specific PCR product, the amounts of enriched sequences, and the library diversity can be obtained for every single SELEX in just 30 min. Compared with current methods, this system can reduce the time for generating a specific PCR product and SELEX, and it is easier to choose the optimal number of cycles for a specific PCR product. In a word, it is a sensitive, simple, and rapid strategy to improve the specificity of the PCR product and make the process of SELEX in a controlled way.

INTRODUCTION

A nucleic acid aptamer is a single-stranded DNA or RNA molecule with high affinity and performs highly specific binding to the target molecule.[1–3] Aptamers are typically selected from random-sequence oligonucleotide libraries in a process termed SELEX.[4,5] SELEX involves iterated rounds of incubation of the library with the target followed by partitioning of target-bound oligonucleotides from target-nonbound oligonucleotides and polymerase chain reaction (PCR) amplification of all collected oligonucleotides until the ratio of target-bound oligonucleotides to target-nonbound oligonucleotides (B/N) reaches a desired value.[6] Remarkably, SELEX fails to select binders in 70% of attempts.[7] One of the main obstacles for SELEX failure is the generation of a non-specific product of PCR.[8] Moreover, another main obstacle is the lack of a sensitive evaluated processing method to monitor the selection in a controlled way.[9]

To minimize the generation of a non-specific product of PCR, the most conventional PCR procedure for SELEX commonly includes two steps: analytical PCR and subsequent amplification PCR.[10–12] The purpose of analytical PCR is to determine the optimal number of cycles for amplification PCR by conducting PCR with a series of cycle numbers. The optimal number is typically the cycle number displaying the better yield of PCR product in the expected position without a PCR by-product being detected. The nature of the non-specific product of PCR (by-products) was studied by Mayer and colleagues.[8] According to their results, PCR by-products were initiated by the partial binding of the primer to complementary bases that appeared on random regions of library

sequences. The partial binding structure was then extended by the polymerase to yield longer DNA products with higher molecular weights than parental library sequences. Because long stretches of such by-products allowed for more efficient annealing during PCR, without proper control, these ever-longer sequences could be preferentially amplified and they eventually dominate the library composition. However, the two-step optimization method still has some problems. First, the commonly used detection methods sometimes do not have enough resolution or sensitivity to detect by-products. For example, agarose electrophoresis is the most commonly used method for choosing the optimal number of cycles for PCR. If we detect the PCR products in optimal cycle via the high-resolution PAGE, clear PCR by-product bands can be identified, which are not detected by agarose electrophoresis.[13] Therefore, by choosing a more sensitive dye or detection method, non-specific bands could be observed from a gel that did not initially show the non-specific bands. Also, in the multiple operations of the two-step PCR in the open environment, pollution contamination and fragment loss of the SELEX library may be caused. Therefore, it is urgent to develop a sensitive, simple, and rapid method to improve the PCR specificity.

Evaluating the SELEX process and optimizing its conditions can increase the selection efficiency in a controlled way.[9] Various attempts have been made to monitor the selection progress of target-specific ligands.[14–18] These assays are summarized in two ways: (1) directly measuring the affinity of every round of the ssDNA pool to the target or (2) assessing the sequence diversity of the pools (convergence of the aptamer species).[19] However, affinity assays suffer from several limitations and drawbacks, especially when there are still a lot of random and non-specific oligonucleotides present in the eluted fractions.[20] For example, the straightforward and most informative way of monitoring is assessing the sequence diversity of the pools. However, it is not applicable to the more random stages of the library in the first few rounds of selection. Affinity assays also cannot provide enough resolution or sensitivity for sensitive SELEX monitoring. Recently, Jeroen *et al.* used reMelting Curve Analysis (rMCA), which, after reannealing under stringent conditions, provides information about enrichment compared to a random library.[20] Luo *et al.* developed a combined strategy that depended on the quantitative polymerase chain reaction amplification curve (AC) and the melting curve analysis (MCA) to monitor the convergence of the aptamer species during the selection progress.[21] Both show that real-time PCR provides a valuable tool for the follow-up of aptamer selection. However, there is still a lack of a method to straightforwardly evaluate every round of the screening process online.

As microfluidic chips offer rapid heat transfer, low thermal inertia, and small thermal mass, there are many researchers concentrating on the operation of PCR in a microfluidic device.[22,23] Ha and Lee developed a microfluidic device where 30 cycles of PCR were created in a polycarbonate substrate. The temperatures were created using two copper heating blocks for denaturation.[24] Salman *et al.* reported a shunting PCR microfluidic device that consisted of a microfluidic PCR chip, a shunting thermal cycler, and a fluorescence detector, and this approach had the advantages of fast cycling times.[25] However, there were few reports on improving the specificity of PCR chips and using PCR chips to monitor each round of SELEX. In this work, we aim to develop a new platform based on the real-time PCR detection chip and the large volume PCR chip to fulfill one-step specific PCR and evaluate the SELEX process. First, compared to the conventional two-step PCR, we found that the optimal number of cycles for generating a specific PCR product was when the slope of the linear amplification period of the real-time PCR curve began to decrease. Second, the time used by the dual-microfluidic amplified system (dual-MAS) was only a quarter of the traditional method. Third, the multifunctional dual-MAS could simultaneously evaluate the SELEX process by providing the important information of the amount of the enriched sequences bound to target and the library diversity. Therefore, it is a sensitive, simple, and rapid strategy to improve the specificity of the PCR product and evaluate the SELEX process.

EXPERIMENTAL

Materials and reagents

SG-2506 borosilicate glass was purchased from Changsha Shuguang Chromium Board Co., Ltd. Dow Corning Sylgard 184 PDMS prepolymer was purchased from Dow Corning Corporation (USA). 2× Taq Master Mix premixed enzyme was purchased from Tiangen Bio (Beijing) Co., Ltd. 2× SYBR® Premix Ex TaqTM was purchased from Takara (Japan). 1× TBE (89 mM Tris, 89 mM boric acid, 2 mM EDTA) and 30% (w/v) acrylamide/methylene bisacrylamide solution were purchased from Shanghai Shenggong Bioengineering Co., Ltd. Dechromic solution is 200 mg/ml ammonium cerium nitrate and 3.5% (v/v) glacial acetic acid mixture. Etching solution was a mixture of 18.6 mg/ml NH_4F, 4.64% (v/v) HNO_3 and 5% HF. Buffer solutions used in this experiment were 1× phosphate buffer saline (PBS) (137 mM NaCl, 2.7 mM KCl, 10 mM $Na_2HPO_4 \cdot 12H_2O$, 2 mM KH_2PO_4, pH 7.4), 1× the mixture of phosphate buffer saline and $MgCl_2$ (PBSM) (1× PBS + 1 mM $MgCl_2$, pH 7.4), 2× PBSM (254 mM NaCl, 5.4 mM KCl, 20 mM $Na_2HPO_4 \cdot 12H_2O$, 4 mM KH_2PO_4, 2 mM $MgCl_2$, pH 7.4), and 1× the mixture of phosphate buffer saline and Tween-20 (PBST) (1× PBS + 0.05% Tween-20, pH 7.4). 1× PBS was purchased from Invitrogen (USA). All reagents were of analytical grade and were not further purified. All aqueous solutions were prepared using ultrapure water (≥18.20 MΩ) from the Millipore system, with some sterilized in a high-temperature sterilizer and then filtered using a 0.22 μm Millipore filter. The ssDNA library and primers used in this work reported by the Yang Xiaohai Group of Hunan University were synthesized and purified by Shanghai Shenggong Bioengineering Technology Co., Ltd. The 80 nt screening library consists of a random sequence of 40 nt in the middle and two ends. Each 20 nt amplification site is composed. The specific sequence is shown in Table S1 in the supplementary material.

Apparatus

The following apparatus were used: LSP04-1A microfluidic injection pump (Baoding Lange Constant-Flow Pump Co., Ltd., China) for liquid operation; PDC-MG plasma cleaning machine (Chengdu Mingheng Technology Co., Ltd., China) for sealing PDMS and glass substrates; bole gel imager (Bole Life Medicine Products (Shanghai) Co., Ltd.) for polyacrylamide gel

electrophoresis imaging acquisition; ESElog fluorescence detector (E470/565 D520/625, Tiangen Biotechnology (Beijing) Co., Ltd.) for collecting fluorescence signal; Pico BSB TC-08 thermocouple temperature recorder (Guangzhou Hongke Electronic Technology Co., Ltd.) for PCR chip temperature data acquisition. GEN4T thermal cycler (Hangzhou Baiheng Biotechnology Co., Ltd.) provides the PCR chip heat source. The lifting and lowering three-dimensional light source fixing frame (Shenzhen Xiexuan Technology Co., Ltd.) was used for the fixation and optical path adjustment of the ESElog fluorescence detector. The DYY-8C electrophoresis instrument (Beijing Liuyi Instrument Factory) was used for polyacrylamide gel electrophoresis. UV- Vis spectra were measured on a Synergy Hybrid Reader (BioTek, USA).

Design of the microfluidic chip

Microfluidic chip preparation process

Microfluidic channel graphics were designed and printed as a $63 \times 63\ mm^2$ film using the Adobe Illustrator cs5 software. The template was overlaid on a photoresist-coated chrome plate for 3.5 min in the UV, rinsed with % (w/v) NaOH for 1 min, and the chrome layer was removed by rinsing in the dechromizing solution for about 3 min. Finally, it was etched at 37 °C for 1.5 h with $HF/NH_4F/HNO_3$ solution. A microfluidic channel template was obtained after aging at 80 °C for 1 h.

Preparation of PDMS channel

The PDMS prepolymer and the curing agent were mixed uniformly at a mass ratio of 10:1, placed in a vacuum desiccator, vacuumed for 30 min to remove bubbles, and then poured onto the prepared template. The PDMS microfluidic channel was obtained after heating at 80 °C for 1.5 h. Finally, the amplification chamber, sample inlets, and sample outlets were punched and treated with a 0.17 μm glass substrate by plasma treatment to form the PCR microfluidic chip.

Chip fixture design

According to the structure of the dual-amplification microfluidic system, the structure and the channel of the corresponding channel inlet, outlet, and reaction chamber were made by the bench driller on the 4 mm PMMA plate. Besides, screw holes corresponding to the bottom heating module were designed at the four corners of the PMMA plate for fixing the PCR chip onto the heating plate.

Fabrication of the dual-MAS

The physical photograph of the dual-MAS is shown in Fig. S1 in the supplementary material. The construction process was as follows: (1) the microfluidic chip was integrated with the thermal cycler. The double-amplification microfluidic chip was fixed to the heated aluminum plate of the temperature cycler by a PMMA clamp through a dense-grain screw. The temperature of the temperature cycler could be set and controlled by computer software. (2) Installation of the fluorescence detector and optical path debugging. The ESElog probe was fixed on the microfluidic chip through a three-dimensional light source holder. Then, the fluorescent focusing light path was aligned by controlling the front and rear up and down adjustment knobs of the three-dimensional light source holder. The optical path could be adjusted by adding an equal volume of 1× ROX Reference Dye II (Takara) to the PCR well to fit the optimal optical path. (3) The connection of the fluid system. The microfluidic syringe pump and the two-channel switching valves were connected to the chip through the pipeline. The switching valve was controlled by computer software. (4) The connection of the temperature recorder. The sensing end of the K-type thermocouple temperature was connected to the inner wall of the PCR chambers and then connected to a Pico thermocouple recorder for on-chip temperature characterization and data recording.

Operation of the dual-MAS

A schematic of the constructed dual-MAS is shown in Fig. 1. The eluted enriched library flows into the microfluidic chip channel from inlet 1 through the syringe pump and is divided into two fluids with a volume ratio of 1:16 when passing through the asymmetric herringbone channel. 25 μl of 2× SYBR Premix Ex TaqTM enzyme [1.25 μM forward primer (FP), 1.25 μM reverse primer (RP)] was injected through Inlet 2, and Inlet 3, 200 μl 2× Taq Master Mix premixed enzyme [1.25 μM tetramethyl-6-carboxyrhodamine (TAMRA)-labeled FP (TAMRA-FP), 1.25 μM Biotin-RP] flowed into a single chamber PCR fluorescence detection unit and large volume PCR amplification unit, respectively. This design is used to ensure that most of the eluted (15/16) enriched libraries are recovered after optimal amplification and are passed to the next round of screening. A small amount (1/16) of the library was mixed with 2× SYBR Premix Ex TaqTM premixed enzyme for qPCR amplification to provide information on the concentration, diversity, and the optimal number of PCR cycles of the enriched library.

Characterization of the dual-MAS

The four-amplification microfluidic system was characterized by fluid distribution, temperature cycling, PCR standard curve, and

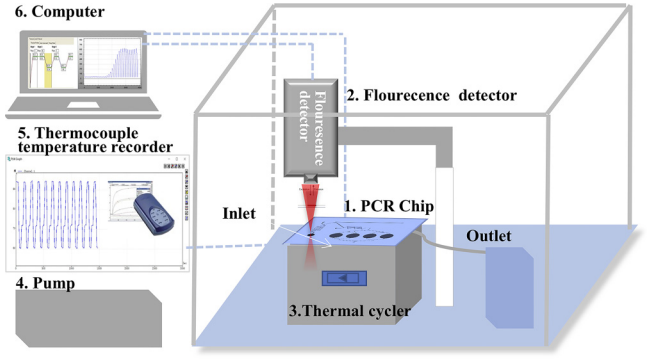

FIG. 1. Illustration of the dual-MAS (dual-microfluidic amplification system). The system mainly contains: (1) PCR chip, (2) fluorescence detector, (3) thermal cycler, (4) pump, (5) thermocouple temperature recorder, and (6) computer.

multi-chamber amplification consistency. (1) Fluid delivery: the eluted enriched library flowed from the inlet 1 into the microfluidic channel. The volume of the solution flowing into the five chambers was measured, and the experiment was repeated three times; (2) the temperature cycle was characterized: thermocouple temperature recording was used to measure the temperature cycle rate inside the chip, record the temperature cycle curve; (3) establish the standard curve: libraries of known concentration in the range of 1 pM to 1 nM were amplified to develop a standard curve, which was repeated three times at each concentration; (4) multi-chamber amplification consistency: by performing the same experiment under the same conditions by placing the fluorescent probes in five PCR chambers respectively, it was possible to characterize the amplification uniformity between different chambers of the same chip.

Optimization of amplification methods

The concentration and diversity of the enrichment library, the method of *in situ* monitoring, and the optimal amplification method were studied. First, we could perform highly sensitive assays on the concentration of enriched libraries (1 pM to 1 nM). In addition, various studies of enriched libraries could be performed by the shape of the qPCR amplification curve. We designed a random library with different fixed sequence content (0%, 5%, 10%, 20%, 40%, 80%, 100%) as the initial template for qPCR amplification to study library diversity and qPCR amplification curves. Also, we studied the quantitative amplification method of PCR. By studying the relationship between real-time PCR amplification curves of different initial templates and polyacrylamide gel electrophoresis, a method for determining the optimal number of amplification cycles of PCR was established.

Screening of aptamers based on the dual-MAS

The PMM-SELEX chip was integrated with the dual-MAS to screen the lactoferrin nucleic acid aptamer. First, after the library was separated from the protein in the negative sieve and the positive sieve channel, the nucleic acid library bound to the target protein in the positive sieve channel was eluted with 425 μl of diethyl pyrocarbonate (DEPC) water at 95 °C, and the enriched library was subjected to double-amplification microfluidics. The fluid was distributed in the chip and premixed with 2× SYBR Premix ExTaqTM (1.25 μM FP, 1.25 μM RP), 2× Taq Master Mix (1.25 μM TAMRA-FP, 1.25 The μM Biotin-RP) enzyme quickly. Finally, the qPCR fluorescence detection system was monitored, and the number of rounds was optimized, and the enriched library was accurately amplified in the large volume PCR chip. The amplified product was a purified and single-stranded library entered the next round of screening.

RESULTS AND DISCUSSION

The principle of the dual-MAS

Figure 2(b) is a schematic diagram of the structure of a dual-MAS. The small-sized chamber (d = 3.5 mm) on the chip is a real-time PCR amplification chamber and four large volume chambers (d = 7 mm). The real picture after the chip is mounted is shown in Fig. 2(a). When the chip is attached to the temperature cycling module, the ESElog fluorescence probe is used to collect data. ESElog fluorescence probes have the advantages of fast acquisition speed, high sensitivity, and easy integration. Before the PCR amplification, we use the movement of the 3D light source holder and adjust the correct focus position of the probe through the 1xROX Reference Dye II (Takara) indication, through the up and down debugging, when the maximum fluorescence signal was reached. Figure 2(a)-(a) is a photo of the fluorescence probe in the data acquisition state. We take a real-time intermittent data acquisition mode (1 time/s), which has the advantage that we can observe whether the denaturation, annealing, and extension steps in the PCR cycle are completed by collecting complete data, especially when the PCR product increases. Incomplete stages can cause a large number of by-products. Figure 2(d) shows the original data of the real-time data. To make the amplification curve more intuitive, we take the average of the ten values in the middle of the extension for 10 s and the number of amplification rounds to obtain the graph of Fig. 2(d). The processing of the data after this experiment was completed as described above. Figure 2(c) is a physical diagram of the integrated system of the microfluidic chip heating module. We use PMMA fixture to make the bottom of the microfluidic chip and the heating module completely fit, achieve a proper heat transfer effect, improve experimental repeatability, and avoid poor heat transfer efficiency caused by deformation of the microfluidic chip.

Characterization of the dual-MAS

The critical factors in the PCR system are the control of the rate of temperature and temperature control accuracy. Figures 3 and 4 show the real-time temperature profile inside the PCR chamber recorded by the thermocouple. The dual-amplification microfluidic chip substrate consists of ultra-thin glass material (0.17 mm) [the real-time temperature profile is Fig. S2(a) in the supplementary material], and the glass substrate (1.0 mm) [Fig. S2(b) in the supplementary material]. Compared with the set temperature, the error is less than 0.3 °C. Also, the ultra-thin glass substrate microfluidic chip (0.17 mm) that was not fixed by the PMMA fixture [Fig. S2(c) in the supplementary material] has a significantly lower temperature rise and fall rate. The reason is that the ultra-thin glass substrate and the PDMS channel can be easily deformed by heat. A gap with an undefined height of the surface of the temperature module is formed, resulting in a lower heat transfer rate and a significant error in the equilibrium temperature and the set temperature. Fixing the chip on the heating module with PMMA plate makes the chip substrate and the heating module fit entirely, which can significantly improve the thermal conductivity and temperature accuracy of the chip. Besides, the volume of the library amplification system in this experiment is larger (200 μl). Therefore, the temperature diffusion in the solution will become the key factor determining the heat transfer rate. The fast temperature change program will not increase the temperature rise and fall of the solution. So, the temperature rise rate used in this experiment is about 1.5 °C/s, and the temperature drop rate is about 1.4 °C. It perfectly matches the heat transfer rate of a large volume PCR system solution and can fully meet the requirements of this experiment.

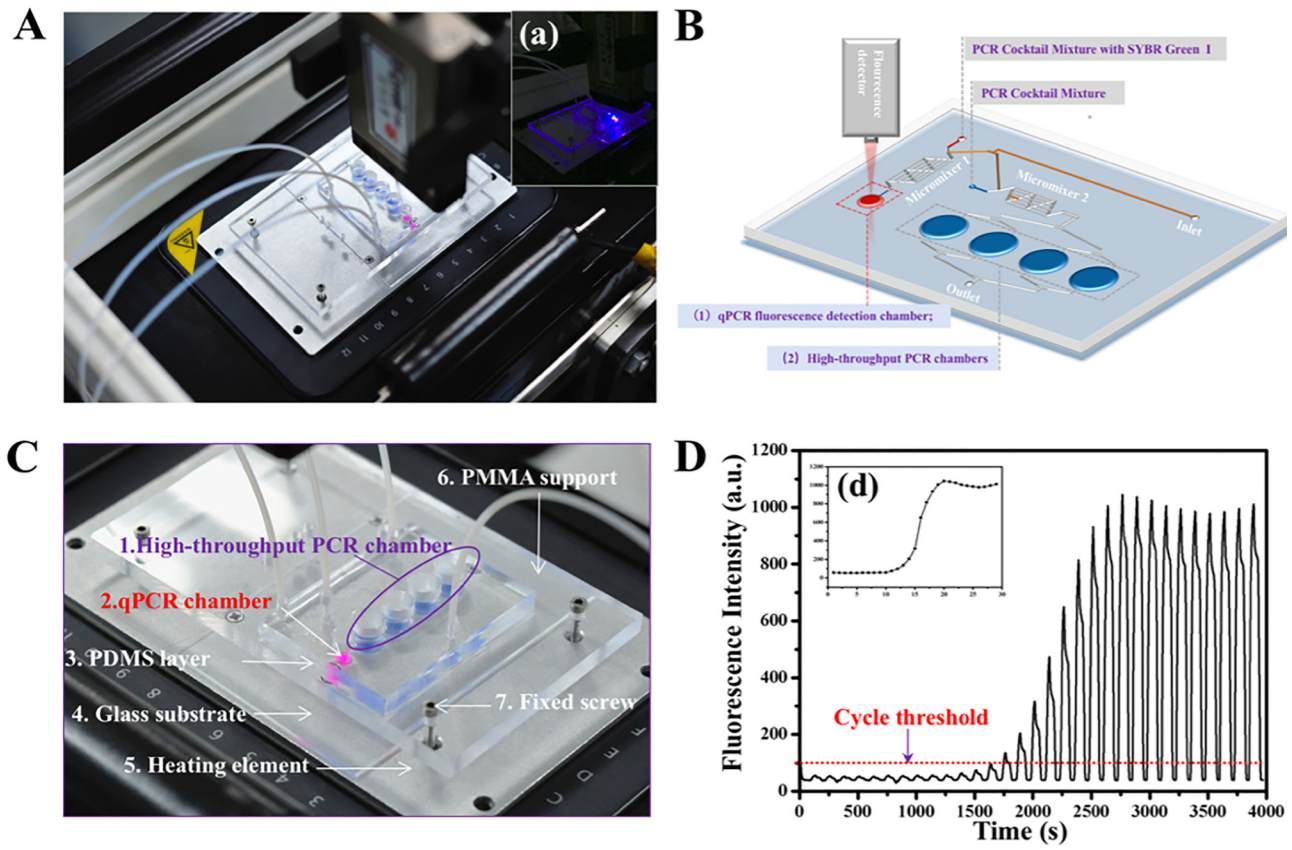

FIG. 2. (a) Top view photograph of the microfluidic chip and (a) inset photograph of the chip placed above the fluorescence measuring system. (b) Diagram of the microfluidic chip. (c) Photo of the experimental setup for a dual-MAS chip. (d) The real-time fluorescence recording curve and converted to (d) real-time amplification curve.

Subsequently, we conducted experiments on the multi-chamber amplification consistency of the microfluidic chip. In this experiment, we performed PCR amplification of random libraries in the concentration range of 1 pM to 1 nM, and each sample was repeated three times. The concentration range of this experiment was selected based on the concentration of the enriched library collected after eluted in the aptamer screen. In general, the number of initial libraries is about 1×10^{14}, and the number of nucleic acid libraries retained after the interaction with the target is about 1.4×10^{7}–1.4×10^{10} and then amplified by PCR about 1×10^{3}–1×10^{6} times as a secondary library. Therefore, the amplification of the microfluidic chip in the concentration range of 1 pM to 1 nM (1.4×10^{7}–1.4×10^{10}) is crucial.

The results obtained in the experiment are shown in Fig. 3(a). We set the Ct value to 100 a.u. The real-time PCR chip we designed has high reproducibility in the range of 1 pM to 1 nM. The initial template concentration was linearly fitted to the Ct value, and a good linear correlation was obtained [Fig. 3(b)]. The linear equation was $y = -2.80x + 26.01$ ($R^2 = 0.997$). Each experiment was performed three times and the RSD (%) was less than 3% for each point. This indicated that the PCR chip had good reproducibility. Therefore, the microfluidic chip designed in this experiment can fully satisfy the accurate quantification of the aptamer screening library concentration. Besides, we have tested the consistency of the amplification curves of the five reaction chambers of PCR. From Fig. 3(d), we can see that the five reaction chambers have good amplification consistency so that we can pass the information obtained by chamber 1 (i.e., the qPCR fluorescence detection chamber) directs the quantification of the PCR amplification chamber to complete optimal amplification of the enriched library. At the same time, we characterized the fluid distribution of the microfluidic chip system. As shown in Fig. S3(a) in the supplementary material, the enriched library after elution (425 μl) is divided into two fluids with a volume ratio of approximately 1:16 when passing through an asymmetric herringbone channel. Both liquids were simultaneously injected. 25 μl 2× SYBR Premix Ex TaqTM enzyme 25 μl (1.25 μM FP, 1.25 μM RP) and 200 μl 2× Taq Master Mix premixed enzyme (1.25 μM TAMRA-FP, 1.25 μM Biotin-RP) flowed into a single chamber PCR fluorescence detection unit and a four-chamber pass through PCR amplification unit, respectively. Therefore, the accuracy of solution distribution directly affects the accuracy of library concentration determination and the concentration accuracy of amplification enzymes, salt ions, deoxy-ribonucleoside triphosphate (dNTPs), etc. in premixed enzymes. As shown in Fig. S3(b) in the supplementary

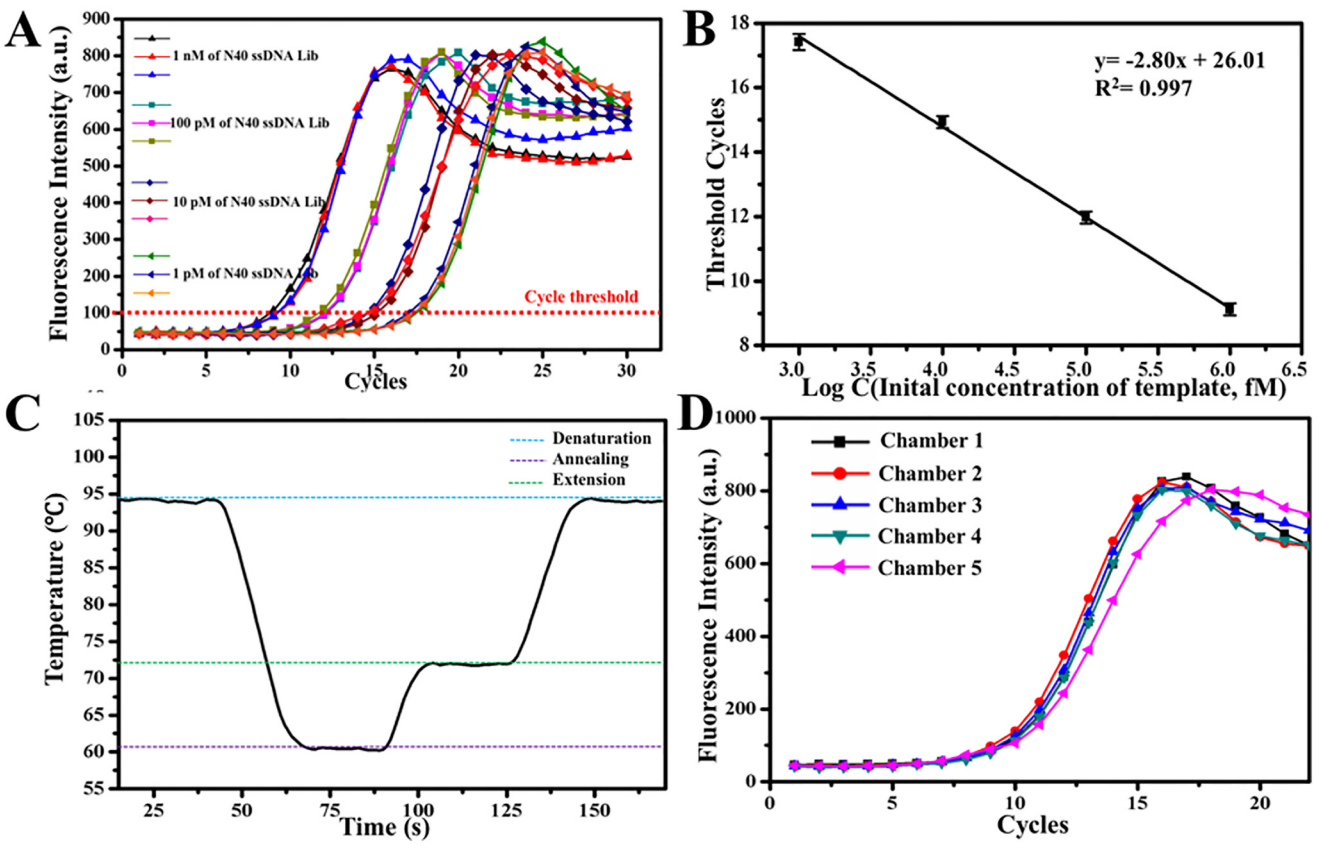

FIG. 3. (a) PCR results from chamber 1 (qPCR fluorescence detection chamber) with the calculated number of ssDNA Lib from 1 pM to 1 nM. Each experiment was performed three times. (b) Extracted standard real-time PCR curve from results in Figs. 3–5 A showing the Ct value as a function of Log (ssDNA Lib concentration). (c) The temperature during one cycle PCR thermocycling. (d) Amplification consistency in PCR chambers 1–5.

material, the channel cross-sectional area of the chevron channel is approximately 1:16. We injected 425, 25, and 400 μl of solution into the three inlets of the microfluidic chip, inlet 1, inlet 2, and inlet 3, respectively, through microfluidic herringbone distribution and two micromixers into five PCR chamber. Finally, we measured the volume of the solution in the chamber, and the average volume of the solution was 51.0, 202, 197, 200, and 196 μl, which indicated proper solution distribution.

Method of one-step PCR

We used the qPCR amplification curve rule to establish a method to obtain the optimal number of amplification rounds. We performed real-time PCR amplification experiments on libraries at four concentrations of 1 pM to 1 nM, respectively. Figure 4(a) is an amplification curve at four concentrations of 1 pM to 1 nM, and we entered linearity during PCR amplification. Each round of amplification products in the amplification phase was taken out, and the number of products and by-products per round was analyzed by 30% polyacrylamide gel electrophoresis. Cycles 12–19 of PCR products were selected from 1 nM product, cycles 15–22 of PCR products were selected at 100 pM, cycles 17–24 of PCR products were selected at 10 pM, and cycles 20–27 of PCR products were selected at 1 pM. Figure 4(b) is a gel electrophoresis pattern of the number of different amplification cycles at each concentration. The optimal number of turns was obtained by comparing Fig. 4(a) with Fig. 4(b). Taking 1 nM as an example, the gel electrophoresis corresponding to each round of PCR products is shown in Fig. 4(b1). From cycle 12, the brightness of the gel electrophoresis target band gradually increased with the increase of the number of amplification rounds. However, after cycle 16, severe by-product bands began to appear. It is more intuitive to see that the number of PCR rounds is slightly higher by the 3D gel electrophoresis pattern [Fig. 4(c1)], which can cause massive formation of by-products. In this case, we select the optimal number of rounds of PCR for 15 rounds, which is the number of rounds at the end of the slope of the linear amplification period of the real-time PCR. We investigated the slope of real-time PCR from cycles 1–15 of PCR. The slope decreased for the first time in cycle 15, and severely reduced in cycle 16. Therefore, we conclude that the optimal number of PCR cycles is the cycles when the slope of the linear amplification period of the real-time PCR begins to decrease. By analyzing the

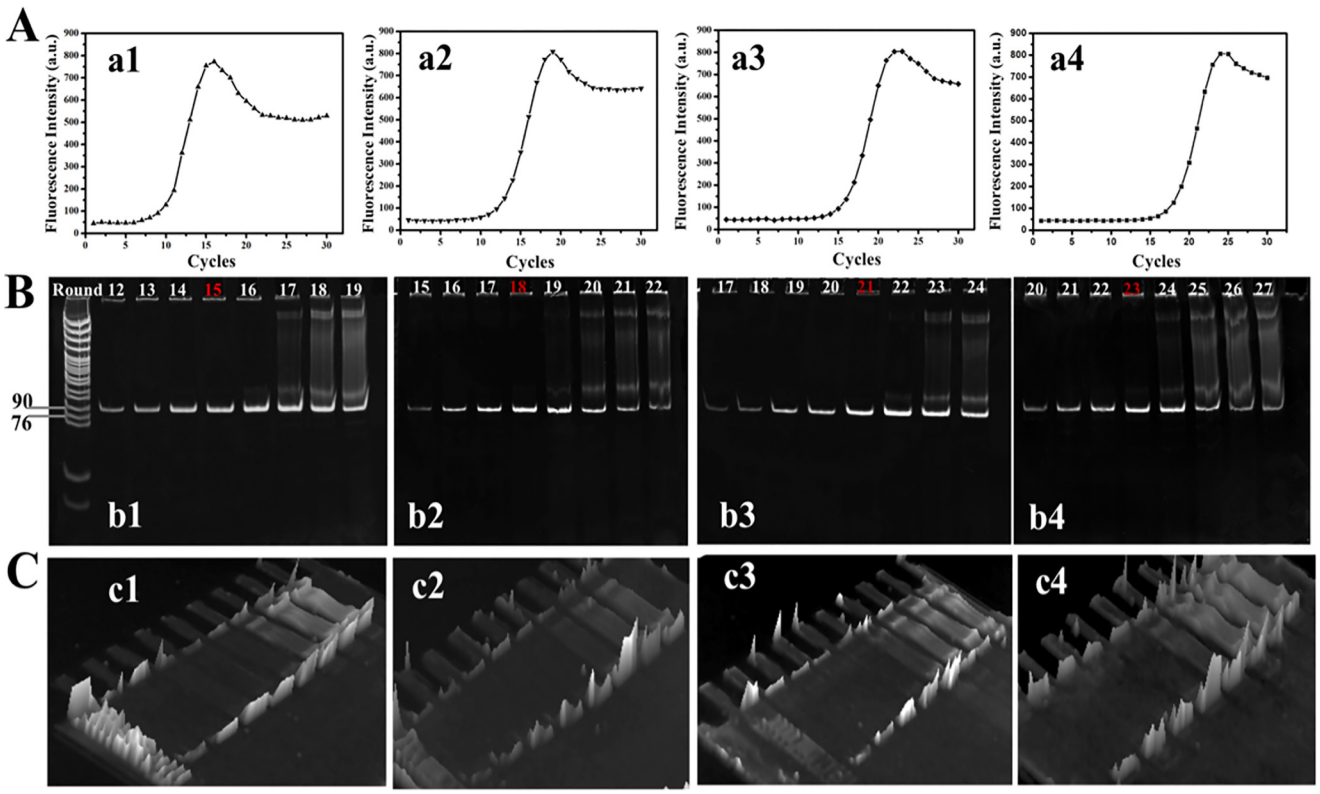

FIG. 4. (a) Illustration of the relationship between qPCR amplification curves with library diversity. (b) The relationship between qPCR amplification curves with a different diversity of the library. (c) 3D gel electrophoresis pattern.

concentration of 100, 10, and 1 pM concentration, and the gel electrophoresis pattern, we obtained the same rule: The optimal number of PCR cycles is the number of the amplification cycle when the slope decreases for the first time in the PCR amplification process. And this method is versatile and suitable for the determination of the optimal number of cycles for different concentrations of library amplification. Also, the time used by the dual-MAS for generating specific PCR product (~30 min) is only a quarter of the traditional method (~2 h). Therefore, it is a sensitive, simple, and rapid method to accomplish optimal PCR in one step.

Method of evaluated SELEX process

We designed the dual-MAS based on a real-time PCR fluorescence detection system to monitor the screening process. (1) Enrichment by calculating the Ct value of the qPCR amplification curve of the enriched library: the concentration of the library and the recovery rate of each round of screening can determine the variation of the screening library with the number of screening rounds. (2) The shape of the real-time PCR amplification curve judges the diversity of the screening library with the increase of the number of screening rounds: Fig. 5 illustrates the use of the shape of the real-time PCR amplification curve to determine the method of screening library diversity. According to related reports,[26,27] when the template nucleic acid sequence has high diversity, the fluorescence intensity increases with the number of PCR amplification products. When a certain number of amplification rounds was reached, the fluorescence intensity no longer increased, but would decrease with the number of amplification rounds. As shown in Fig. 5(a)-(a), this phenomenon is mainly caused by the hybridization of heterologous single-stranded DNA during the amplification process and form an "empty shell structure" that cannot be completely paired, resulting in the inability of the fluorescent molecules to intercalate. The structure increases with the number of amplification rounds. As shown in Fig. 5(a)-(b), when the amplified stock is in a weaker diversity or a single amplified fragment, the fluorescence intensity tends to increase slowly after a certain number of rounds of amplification, and no fluorescence decline occurs. For the first time, we used the real-time PCR to study this rule. We prepared different ratios of known single strands (0%, 5%, 10%, 20%, 40%, 80%, and 100%) mixed with random libraries to study library diversity, and the variation curve of the amplification curve, as well as the rule for monitoring the diversity of the aptamer screening were obtained.

As shown in Fig. 5(b), the amplification curve of the 100% random library showed a severe downward trend. As the

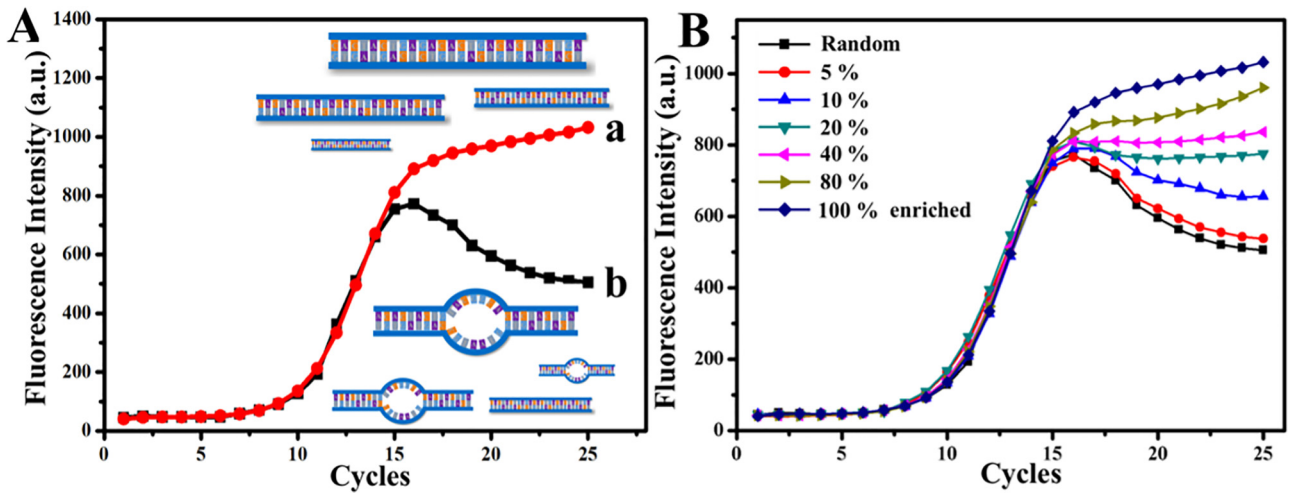

FIG. 5. (a) Illustration of the relationship between the on-chip qPCR amplification curve with the library diversity. (b) The relationship between the on-chip qPCR amplification curve with a different diversity of the library.

single-strand ratio increased, the decreasing trend gradually slowed down. When the single-strand ratio reached 40%, amplification was performed. The curve no longer drops. When it comes 80%, the fluorescence intensity increases with the number of screening rounds, while in 100%, the amplification curve is a gently increasing curve. This gradual increase at the beginning of PCR was mainly caused by the reduced enzyme activity in the PCR system, the continuous consumption of dNTPs, primers. Therefore, through this experiment, we can use the dual-MAS to monitor the diversity of the screening library *in situ* qualitatively. This information can provide valuable information for when to end the screening experiment. Also, the profoundly enriched screening library facilitates the selection and classification of the resulting large number of sequences after cloning, sequencing, and repeated sequence acquisition and high-throughput sequencing.

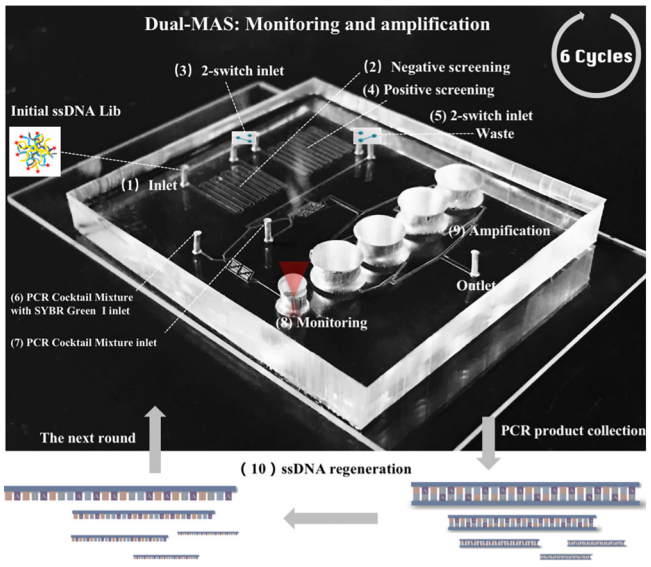

FIG. 6. The principle of the integrated SELEX on dual-MAS with PMM-SELEX. This system contains: (1) inlet 1, (2) negative screening channel, (3) two-switch inlet, (4) positive screening channel, (5) two-switch inlet, (6) PCR cocktail mixture with SYBR Green I inlet, (7) PCR cocktail mixture inlet, (8) monitoring chamber, (9) amplification chambers, and (10) ssDNA regeneration.

Screening of aptamers based on dual-MAS

To characterize the availability of dual-MAS in aptamer screening systems, we have established Dual-MAS and PMM-SELEX chip integrated aptamer screening platforms. The screening diagram of the screening platform is shown in Fig. 6. Firstly, the library was injected from the inlet (1) into the screening channel and interacted with the negative protein and the target protein in the negative sieve (2), the positive sieve channel (4), respectively. After finishing, the positive channel was washed with buffer, and the sequence bound to the target protein was eluted with 425 μl of DEPC water at 95 °C to form an enriched library. The enriched library was directly passed through the double-amplification microfluidic system chip inlet (5). After entering the chip, the distribution of enriched library solution was completed in the amplification chip and the library was rapidly mixed in-line with 2× SYBR Premix Ex TaqTM premix enzyme and 2× Taq Master Mix. Finally, monitoring and PCR cycle optimization was performed on the real-time PCR fluorescence detection chamber, and the enriched library was efficiently amplified in the amplified region of the quantified library. The amplified product was obtained by the above method and then entered the next round of screening and amplification. It can be seen that the dual-MAS can

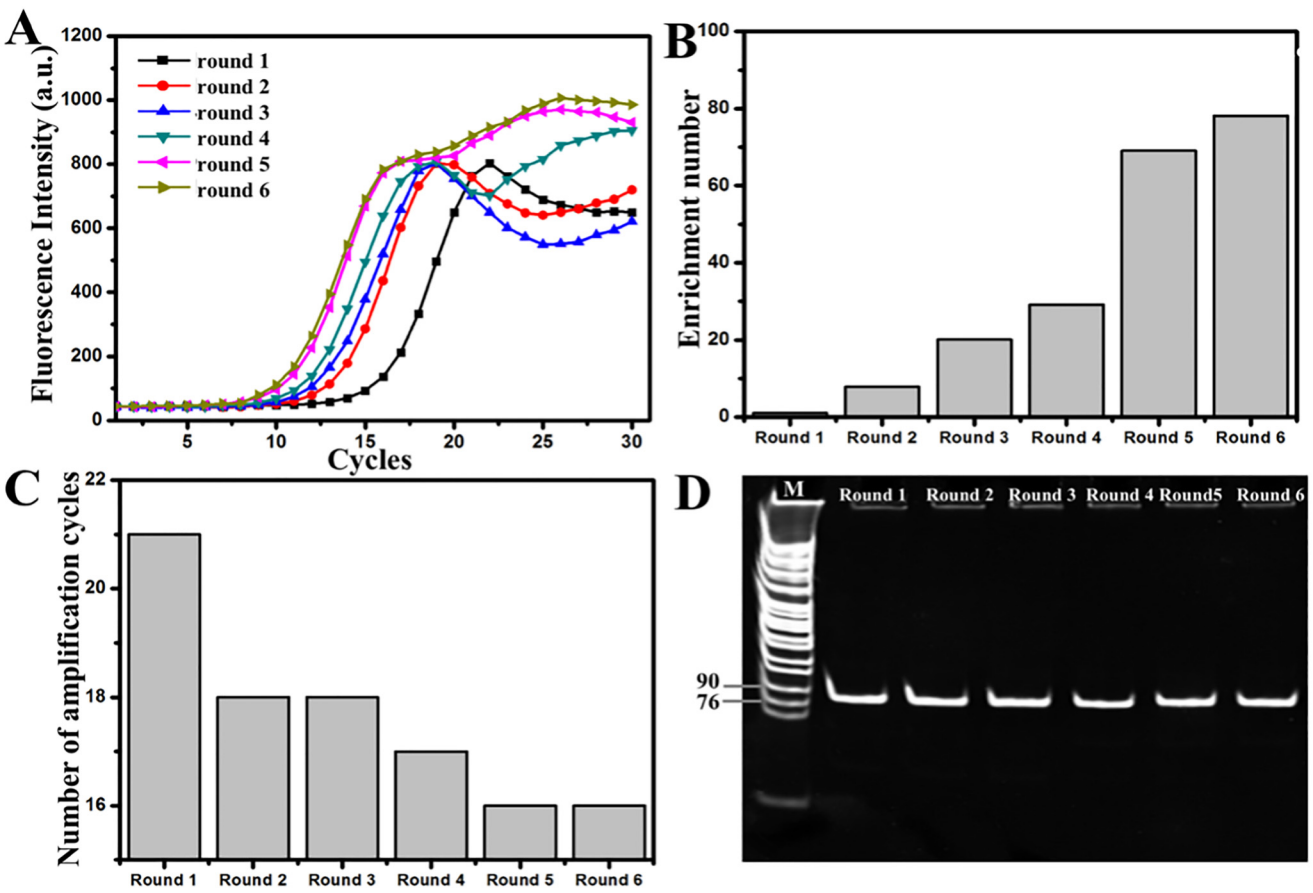

FIG. 7. (a) Monitoring aptamer screening process based on the qPCR amplification curve. (b) Enrichment number of Lib from round 1 to round 6. (c) Optimal number of PCR amplification for every SELEX round. (d) The gel electrophoretogram of PCR products from round 1 to round 6.

be integrated with the microfluidic aptamer screening to complete online amplification and multi-information monitoring of the library.

The dual-amplification microfluidic chip system was used as a screening, monitoring, and amplification method, and six rounds of aptamer screening were completed in only 3 days. The screening results are shown in Fig. 7. It can be seen from Fig. 7(a) that as the number of screening rounds increases, the Ct of real-time PCR decreases continuously, which indicates an increase in the number of nucleic acid libraries that specifically bind to the target protein during the screening process. Besides, with the increase of the number of screening rounds, from the fourth round, the fluorescence of the real-time PCR curve began to decrease. When the fifth and sixth rounds were reached, the fluorescence of the real-time PCR amplification curve no longer decreased. At this time, the diversity of the library was greatly reduced. Subsequent work such as cloning and sequencing could be carried out. We substituted each round of screening Ct values into the standard curve concentration formula, $y = -2.80x + 26.01$, to obtain the concentration of each round of the enriched library that specifically binds to the positive screen target. Using the concentration obtained after the first round of screening as the initial concentration, we calculated the enrichment factor for each round of screening from the second round. The multiple enrichment results are shown in Fig. 7(b). It can be seen that after six rounds of screening, we obtained about 80 times enrichment compared to the result of the first round of selection. Therefore, the number of rounds of optimal PCR is also decreasing from the optimal round of 21 cycles in the first round to the optimal round of 16 cycles in the sixth round [Fig. 7(c)]. Moreover, we identified each round of PCR products by polyacrylamide gel electrophoresis [Fig. 7(d)]. As a result, it was found that the target band of each round of PCR product was bright, the amplification yield was high, and no by-product appeared. Therefore, it is proved that the optimal PCR method of the dual-MAS has very high accuracy and reliability. Also, we compared the monitoring method based on the dual-amplification microfluidic chip system with the fluorescence *in situ* scanning and monitoring method, and we have reported and obtained the same results (Fig. S4 in the supplementary material). It can be seen that both monitoring methods indicate that the degree of enrichment of

the screening library reaches dynamic saturation after reaching the fifth and sixth rounds. Therefore, the monitoring method based on the dual-MAS is accurate, reliable, and fast and can achieve the advantages of optimal amplification of the enriched library.

CONCLUSION

The dual-microfluidic amplified system (dual-MAS) is a sensitive, simple, and rapid method to accomplish analytical PCR and subsequent amplification PCR in one step. We found that the optimal number of cycles for generating a specific PCR product was when the slope of the linear amplification period of the real-time PCR curve began to decrease, and the time used by the dual-MAS for generating a specific PCR product was reduced to 30 min. In addition, each experiment was repeated three times, and the results showed that the chip had good reproducibility. The multi-functional dual-MAS could be used for evaluating the SELEX process by providing critical information on the amounts of the enriched sequences bound to the target and the library diversity in every round of SELEX simultaneously. After integrating the dual-MAS with PMM-SELEX, a specific PCR product, the amounts of the enriched sequences bound to the target and the library diversity were obtained for every single SELEX in just 30 min. Therefore, it has been proven to be a sensitive, simple, and rapid strategy to improve the specificity of the PCR product and make the process of SELEX in a controlled way. This dual-MAS can be used for performing one-step specific PCR and monitoring the SELEX process online, and further promoting the rapid and accurate screening of aptamers for multiple targets.

SUPPLEMENTARY MATERIAL

See the supplementary material (Table S1) for the detailed DNA sequence information used in this work. Refer to Fig. S1 for photograph of the dual-microfluidic amplified system, Fig. S2 for the characterization of the performance of microfluidic thermalization, Fig. S3 for the diagram of the microfluidic channels, Fig. S4 for and the related results of SELEX on microfluidic chip.

ACKNOWLEDGMENTS

This work was supported by the National Natural Science Foundation of China (NNSFC) (Nos. 21775068 and 21974066) and the Excellent Research Program of Nanjing University (No. ZYJH004). Zhoumin Li acknowledges the University Cyan Blue Engineering Program of Jiangsu Province (No. 0010392001) and the Teaching Reform Project of Nanjing University Jinling College (No. 0010522020).

DATA AVAILABILITY

The data that support the findings of this study are available within the article and its supplementary material.

REFERENCES

[1]D. H. Shangguan, Y. Li, Z. Tang, Z. C. Cao, H. W. Chen, P. Mallikaratchy, K. Sefah, C. J. Yang, and W. Tan, Proc. Natl. Acad. Sci. U.S.A. **103**, 11838–11843 (2006).
[2]G. Mayer, Angew. Chem. Int. Ed. Engl. **48**, 2672–2689 (2009).
[3]M. Mascini, I. Palchetti, and S. Tombelli, Angew. Chem. Int. Ed. Engl. **51**, 1316–1332 (2012).
[4]D. L. Robertson and G. F. Joyce, Nature **344**, 467–468 (1990).
[5]C. Tuerk and L. Gold, Science **249**, 505–510 (1990).
[6]A. T. H. Le, S. M. Krylova, M. Kanoatov, S. Desai, and S. N. Krylov, Angew. Chem. Int. Ed. Engl. **25**, 2739–2743 (2019).
[7]J. Zhou and J. Rossi, Nat. Rev. Drug Discov. **16**, 181–202 (2017).
[8]F. Tolle, J. Wilke, J. Wengel, and G. Mayer, PLoS One **9**(12), e114693 (2014).
[9]J. Müller, O. El-Maarri, J. Oldenburg, B. Pötzsch, and G. Mayer, Anal. Bioanal. Chem. **390**, 1033–1037 (2008).
[10]M. Haghighi, H. Khanahmad, and A. Palizban, Molecules **23**, 715–722 (2018).
[11]Q. Wang, W. Liu, Y. Xing, X. Yang, K. Wang, R. Jiang, P. Wang, and Q. Zhao, Anal. Chem. **86**, 6572–6579 (2014).
[12]X. Liu, H. Li, W. Jia, Z. Chen, and D. Xu, Lab Chip **17**, 178–185 (2016).
[13]T. Wang, C. Chen, L. M. Larcher, R. A. Barrero, and R. N. Veedu, Biotechnol. Adv. **37**, 28–50 (2019).
[14]W. Yoshida, E. Mochizuki, M. Takase, H. Hasegawa, Y. Moritaa, H. Yamazakib, K. Sodea, and K. Ikebukuroa, Biosens. Bioelectron. **24**, 1116–1120 (2009).
[15]C. Wang, G. Yang, Z. Luo, and H. Ding, Acta Biochim. Biophys. Sin. **41**, 335–340 (2009).
[16]X. Cao, S. Li, L. Chen, H. Ding, H. Xu, Y. Huang, J. Li, N. Liu, W. Cao, Y. Zhu, B. Shen, and N. Shao, Nucleic Acids Res. **37**, 4621–4628 (2009).
[17]B. Hwang and S. I. Lee, Biochem. Biophys. Res. Commun. **290**, 656–662 (2002).
[18]M. Berezovski, A. Drabovich, S. M. Krylova, M. Musheev, V. Okhonin, A. Petrov, and S. N. Krylov, J. Am. Chem. Soc. **127**, 3165–3171 (2005).
[19]A. Ozer, J. M. Pagano, and J. T. Lis, Mol. Ther. Nucleic Acids **3**, e183 (2014).
[20]V. Jeroen, L. Karen, V. Katrijn, L. Jeroen, and M. Luc, Analyst **139**, 589–595 (2014).
[21]Z. Luo, L. He, J. Wang, X. Fang, and L. Zhang, Analyst **142**, 3136–3139 (2017).
[22]C. D. Ahrberg, A. Manz, and B. G. Chung, Lab Chip **16**, 3866–3884 (2016).
[23]L. Chen, A. Manz, and P. J. Day, Lab Chip **7**, 1413–1423 (2007).
[24]M. L. Ha and N. Y. Lee, Food Control **57**, 238–245 (2015).
[25]A. Salman, H. Carney, S. Bateson, and Z. Ali, Talanta **207**, 120303 (2020).
[26]C. Hu, Z. Yang, Z. Song, L. Xiao, and Y. He, RSC Adv. **10**, 14944–14952 (2020).
[27]T. S. Kang, Trends Food Sci. Technol. **91**, 574–585 (2019).